Frontiers in Economics and Management Volume 2 Issue 8, 2021
ISSN: 2692-7608 DOI: 10.6981/FEM.202108_2(8).0027

Research and Analysis on the Capacity of Hong Kong-Zhuhai-Macao Bridge under the Influence of Crosswind

Chongchi Zeng

International college of Changsha university of science and technology, Changsha, China.

zengchongchi@foxmail.com

Abstract

Hong kong-zhuhai-macao bridge is one of China's national project, its important value of bridge design, this article in view of the Hong Kong and Macao bead bridge bridge design methods, Firstly, this paper studies the maximum speed when the vehicle turns on the cross-sea bridge, establishes the wind speed model under different circumstances, and obtains the maximum speed of the vehicle on the cross-sea bridge under different weather conditions. The results show that the crosswind safety of sedan vehicles is the best, followed by no-load medium buses and container trailers, and the crosswind safety of minivan is the worst. Considering the analysis results, it is suggested that the equivalent wind speed of the bridge deck is equal to 20 m/s as the safe wind speed standard of the bridge deck.

Keywords

Bridge; Vehicle Speed; Traffic Capacity; Different Vehicle Models.

1. Introduction

Remarkable subject of hong kong-zhuhai-macao bridge project has been completed, Hong Kong in the east, west zhuhai and macau, the 55 km hong kong-zhuhai-macao bridge, is the most complex on the history and technology of China, and one of the highest standards of engineering construction requirements, also is the world's longest cross-sea bridge, is Britain's the guardian as the "new seven wonders of the world".

Fig. 1 Hong Kong-Zhuhai-Macao Bridge in full view

In this paper, Firstly, this paper studies the maximum speed when the vehicle turns on the cross-sea bridge, establishes the wind speed model under different circumstances, and obtains the maximum speed of the vehicle on the cross-sea bridge under different weather conditions. [1-3]

ISSN: 2692-7608 DOI: 10.6981/FEM.202108_2(8).0027

2. At maximum speed in the transition phase

We must first understand the basic structure of the bridge, take into account the customs and traditions of different places (driving on the left in Hong Kong and Macao while driving on the right in mainland China), and realize the natural transition of traffic habits between the two sides by turning to the overpass. [4,5] The picture below is the turn overpass, and we can also see the specific structure of the turn overpass intuitively. Popular said Hong Kong-ZhuHai-macao bridge is to use the overpass to implement the left sides of the natural, when we go to Hong Kong from zhuhai we started driving on the right, and all the way to Hong Kong when they found a reminds us the right way of driving into the way of driving on the left side of the street, as the natural route after excessive to drive on the left side of the way. The total weight of the car ranges from 1000kg to 3000kg. The transition principle of cars on the Hong Kong-Macao - Zhuhai Bridge is shown in the figure below.

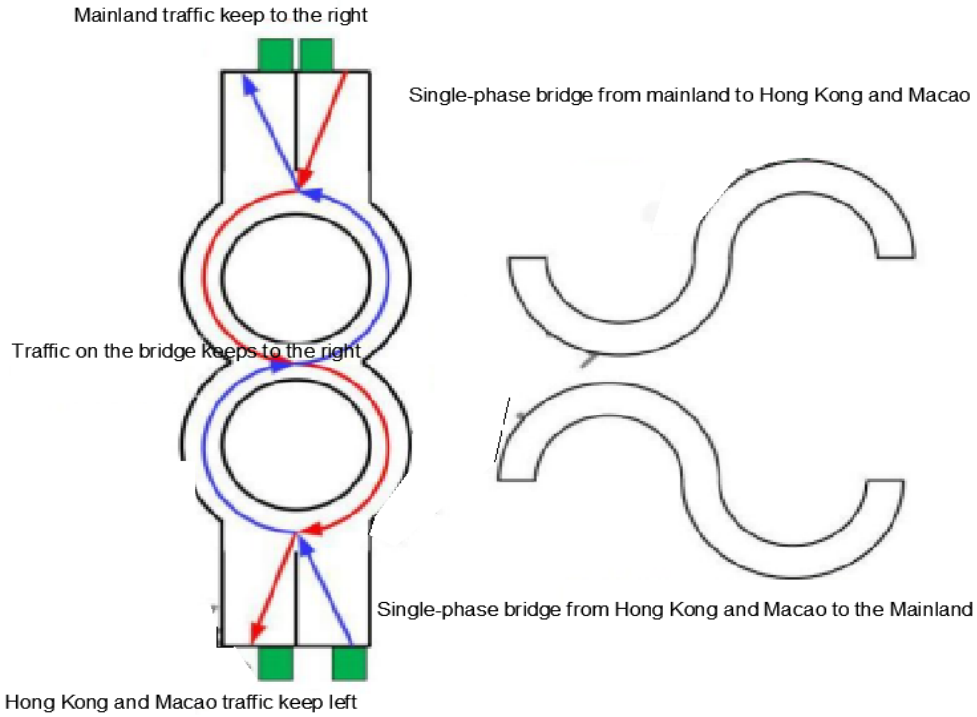

Fig. 2 Diagram of traffic transition on the bridge

If the whole car is taken as the analysis object, it will be very complex and difficult to analyze and solve. It is therefore suggested to consider the car as an ideal model.

Drivers who often drive on the expressway are classified as Group A, and drivers who do not often drive on the expressway are classified as Group B. In addition, the influence of overtaking and non-overtaking are considered, and the following figure is drawn.

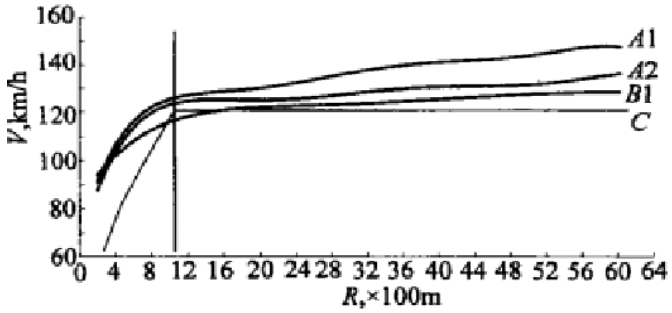

Fig. 3 Comparison of R-V relations under various conditions

ISSN: 2692-7608 DOI: 10.6981/FEM.202108_2(8).0027

The figure shows the relationship between turning radius and speed under different circumstances. In this figure, curve A1 is the R-V relationship of driving group A under the condition of no overtaking, curve A2 is the R-V relationship of driving group A under the condition of overtaking, curve B 1 is the R-V relationship of driving group B under the condition of no overtaking, and curve C is the R-V relationship provided by the specification.

As can be seen from the figure, curves A1 and A2 are consistent in shape. In terms of size, A2 with overtaking effect is always below A1 without overtaking effect from the beginning to the end, and A2 with small radius is about 3-4km /h smaller than A1, and A2 with large radius is about 10-12km /h smaller than A1. Compared with A1 and A2, First, the shape is inconsistent, that is, B1 is much flatter than A1 and A2; Secondly, in terms of size, except for the intersection of the three curves within the radius less than 350m, other parts B1 are lower than A1 and A2, and the driving group A1 even under the influence of overtaking, Analysis of the Relationship between the Radius of the Flat Curve of the Expressway and Vehicle Driving Speed On the curve with the radius of Zhengke greater than 350m, the speed of the driving group B is still about 5km/h higher than that of the driving group B without overtaking.

What needs special analysis is the left-hand curve of the perpendicular to R =1 000. Take curve B1, which is close to the design velocity curve C, as an example.

$$\mu = \frac{V^2}{127R} \pm i \tag{1}$$

The relation curves of velocity V and transverse force coefficient μ with a radius from 200m to 1000m corresponding to curves B, 1 and C can be plotted, as shown in the figure below. In the figure, curve D1 corresponds to curve B1, curve D2 corresponds to curve C, and curve D3 is the recommended value for highway design in the United States. [6-8]

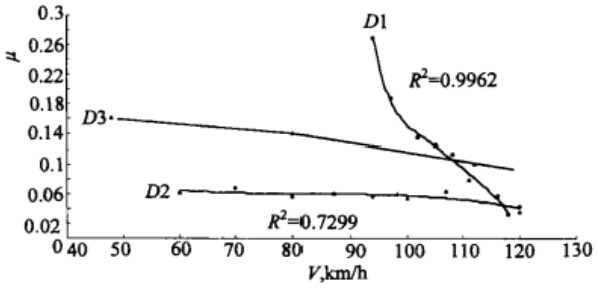

Fig. 4 V-μ relation curve comparison

As can be seen from the figure above, curve D1 has a very steep shape, which is basically above curve D2. It starts roughly from R =900m. As the radius becomes smaller, the difference between the two in the vertical direction, i.e. the difference of the transverse force coefficient μ, becomes larger and larger. Although the curve D3 recommended by the American highway design is generally higher than the curve D2 recommended by the Chinese highway design code, compared with the curve D1, the part of D3 with the radius less than 800m is still much lower.

3. Wind speed influence models for different vehicles

Assume that the maximum typhoon is no more than level 16, and the maximum speed of the vehicle is 100km/h. We should be clear about the concept of the main body of the bridge: the so-called main body of the bridge is the whole of the bridge. So we do a simple force analysis and we know that the most extreme case is when the wind is acting exactly the opposite of the centripetal force on the car in a turn. [9]

Considering that when a car is driving on a curve, under the combined action of lateral wind force and inertia force, the lateral force may exceed the ground lateral adhesion limit, resulting

ISSN: 2692-7608 DOI: 10.6981/FEM.202108_2(8).0027

in lateral slip of the car and loss of normal driving ability. This is a dangerous driving situation that may occur under the action of wind on the bridge deck. The force analysis under this dangerous driving situation is shown in Figure 1, where U is the speed; Fy is the lateral force; F crosswind refers to lateral wind force; R is the turning radius; G is vehicle weight; α is the longitudinal slope of the road; α 'is the lateral slope of the road; Hg is the height of the center of mass; Hw is the height of crosswind operation point; Fz 1 'is left wheel charge; Fz 'is right wheel load; B is the wheelbase.

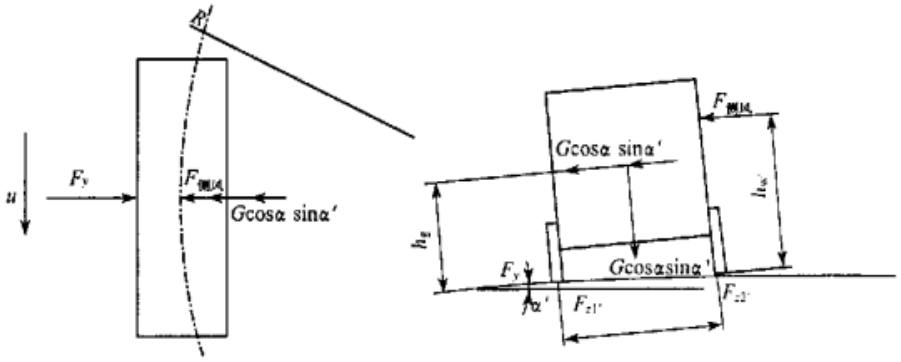

Fig. 5 Dynamic analysis of car on curve in side wind

In order to ensure the normal running of the vehicle, the lateral interference force is required to be less than the lateral adhesion limit, i.e

$$G_{cos\,a\,sin\alpha'} + m\mu^2/R + F_{\text{Cross wind}} \le G\mu_y\, cos\, a\, cos a' \quad (2)$$

$$F_{\text{Cross wind}} = C_{Fs}\tau\rho A V^2{}_{res}/2 \quad (3)$$

$$v_{res} = w^2 + u^2 \quad (4)$$

Where CFS is the vehicle crosswinds coefficient, τ is the resultant inflow Angle, ρ is the air density, A is the upwind area of the vehicle, V res is the resultant velocity, W is the wind speed, and μy is the lateral adhesion coefficient of the ground.

For container semi-trailers, the risk analysis of lateral slip of the whole vehicle is the same as that of buses and cars. However, considering that semi-trailers can rotate around the pin shaft, there is another dangerous situation of this vehicle under the action of crosswind, that is, the wheels on the semi-trailer may slip first under the action of crosswind. The force in this case is shown in the figure. In the formula, FZ3 is the ground normal action reaction force on the semi-trailer wheel.

$$(L_d - c)m2u^2/R + F_{crosswind}(L_d - c - es_2) \le F_{z3}\mu_y L_d \quad (5)$$

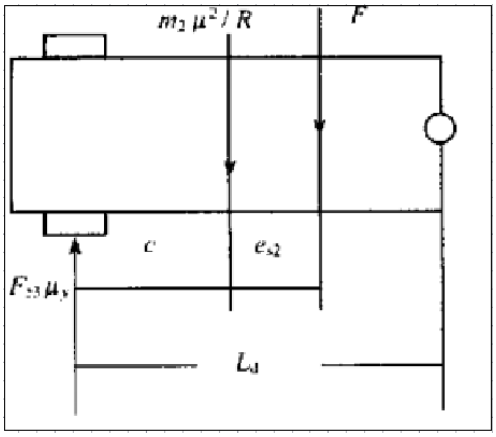

Fig. 6 Force analysis of container semitrailer under crosswind and bend

ISSN: 2692-7608 DOI: 10.6981/FEM.202108_2(8).0027

LD is the distance between the axle of the semi-trailer and the hinge point; ES2 is the distance between the semi-trailer wind power point and the center of mass; C is the distance between the center of mass of the semi-trailer and the axle; F crosswind 2 refers to the lateral wind force acting on the semi-trailer; F is rolling resistance; Hw2 is the height of the wind point on the semi-trailer.32

A certain type of car, mini bus, medium bus and standard container trailer were selected as representatives, among which the mass and side area ratio of mini bus and large and medium bus were significantly different, so the crosswind sensitivity was different. The mass of ordinary truck is higher than that of medium-sized bus, but the lateral aerodynamic force is much smaller because the lateral area is much smaller than that of medium-sized bus, so the crosswind safety of ordinary truck is much better than that of medium-sized bus. The crosswind safety of container trailer is the most unfavorable, which is the focus of the author's analysis.

Tab. 1 Parameter Values of Typical Vehicle Types

Models	Quality	Orthographic area	Height	Width
Cars	1 140	2. 05	1. 40	1. 70
minivans	970	2. 30	1. 90	1. 48
Medium-sized coach	7 100	5. 55	2. 90	2. 25
Container trailer	17 340	8. 89	4. 29	2. 48

Clu0.07 + 0.02b was measured in the wind tunnel test of the car model, so the parameter KCl of the car was 0.02 (B) -1 in the wind speed standard analysis. The lift coefficient of passenger cars and box trailers is much larger than that of passenger cars, and the overall value is almost 2 times that of passenger cars. Therefore, in the standard analysis of wind speed for passenger cars and trucks, KCl = 0.04 (b) -1 is taken.

The coefficient kCS of the lateral force coefficients of car and minivan are 0.0034 (b) -1 and 0.071 (b) -1 respectively, which are fitted by the wind tunnel test results. For passenger cars or freight cars with sides close to rectangles, the value of coefficient KCs increases in direct proportion with the length-height ratio and width-height ratio. Rylski recommends the following formula for approximate calculation of the lateral force coefficient.

$$kcs = (0.005 + 0.0019nf)\frac{M}{A} \tag{6}$$

Where: M is the lateral area; NF is a factor that needs to be estimated according to the KCS values measured by automobile tests similar to the model calculated. Using Equation (5), it is estimated that the KCS value of medium bus is 0.10 ~ 0.18 (b) -1. Based on the principle of engineering safety, the upper limit of KCS value of both bus and container trailer is 0.18 (b) -1. The proportional coefficients between aerodynamic lift and drag coefficients and wind direction Angle of the four representative models are shown in the table below.

As for the longitudinal wind disturbance, as long as the disturbance force is within the driving limit of the vehicle, the driver can overcome it by manipulating the accelerator pedal. As for crosswind interference, although the interference force does not exceed the driving limit of the car, it is easy to cause the car to deviate from the normal driving route. Only by correcting the influence of wind by the driver's steering wheel, can the driver maintain the original driving direction. But if the yaw speed, omega r, is too high for the driver to correct, the car could spin sharply, causing it to skid or roll over. It is also possible to deviate from the lane due to the driving route is too large, and there is a risk of collision with the car in the adjacent lane, thus endangering the safety of driving. In this condition, the time history of yaw velocity ωr is often used to analyze and evaluate the driving stability of vehicles under crosswind action. The yaw

ISSN: 2692-7608 DOI: 10.6981/FEM.202108_2(8).0027

speed omega r will affect the route. As shown in the figure below, Fc is the centrifugal inertia force.

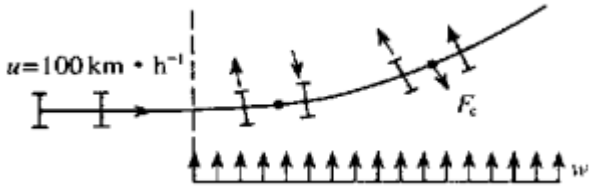

Fig. 7 Side wind' s inf luence on the driving stability

For the car, a two-degree-of-freedom model is established, and the force analysis is shown in the figure below. wr is the yaw angular velocity; V is the lateral velocity; μW is the crosswind moment; FY1 is the front wheel side force; FY2 is the rear wheel side force. According to the following figure, the differential equations of motion can be written:

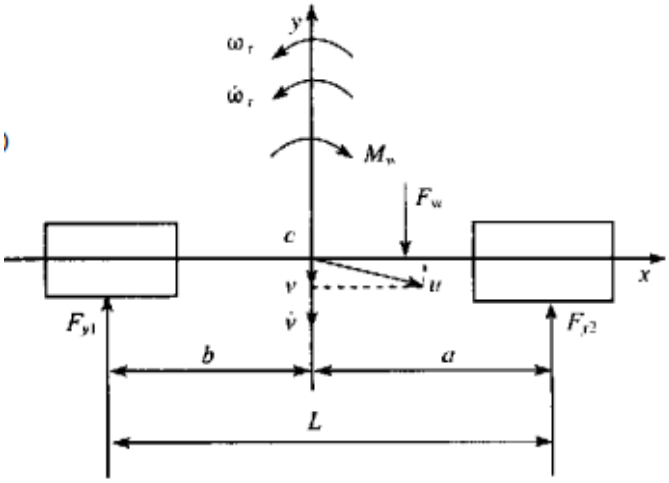

Fig. 8 Vehicle model of 2 freedom degree

$$\begin{cases} (k_1+k_2)\frac{v}{\mu}+\frac{1}{\mu}(ak_1-bk_2)w_r = F_w + m(\dot{v}+uw_r) \\ (ak_1-bk_2)\frac{v}{\mu}+\frac{1}{\mu}(a^2k_1+b^2k_2)\omega_r = M_w + I_z w_r \\ w_r = \dot{\theta} \end{cases} \tag{7}$$

4. Maximum capacity model of bridge

Based on the assumption that the maximum speed of the bridge is 100km/h, the capacity of HZMB is built by considering the factors such as vehicle safety, weather conditions, traffic accident handling and traffic control. It also gives the time for vehicles to cross the bridge at maximum capacity (without considering the occurrence of traffic accidents).

For long-span Bridges in southeast coastal areas of China, snow and ice covered roads rarely appear, while strong wind and rainfall often occur simultaneously. Therefore, based on wet roads, safe driving wind speed standards at different speeds are summarized, as shown in Table 3. It is very difficult to establish a clear safe speed standard for traffic management of Bridges. The speed standard of Redheugh Bridge in the UK is 20 m/s, while the speed standard of Severn Bridge is 16m/s. The main reason why the speed standard is not uniform is not only the factor that affects traffic safety, but also the wind speed. There are also wind direction, wind frequency, vehicle type ratio, traffic management measures and drivers' driving habits.

ISSN: 2692-7608 DOI: 10.6981/FEM.202108_2(8).0027

Tab. 2 Wind Speed of Saf ety Driving Standard of Typical Vehicle Types

Models	The speed of travel at different wind speeds				
	100	80	60	40	20
Cars	30. 5	32. 5	34. 0	34. 0	34. 0
minivans	15. 5	17. 5	19. 0	20. 0	20. 0
Medium-sized coach	19. 5	22. 0	23. 5	24. 3	24. 3
Container trailer	17. 0	20. 0	22. 0	23. 5	23. 5

The probability model of the wind speed on the bridge deck consists of three parts, which are derived from the meteorological observation data near the bridge location and the analysis of the wind environment on the bridge deck. Firstly, the probability model of the wind speed at the reference height Z R is established by the observation data of the wind speed at the weather station near the bridge location. (2) The wind velocity profile of the bridge was fitted by the gradient wind velocity observation data, and the wind velocity relationship between the reference height and the bridge deck height was established. (3) Analyze the bridge deck wind environment and determine the relationship between the bridge deck equivalent wind speed and incoming wind speed.

The variation of wind speed of natural wind is random, but the distribution of extreme wind speed conforms to a certain probability model, in which the function commonly used to describe the probability distribution of wind speed is extreme value type one.

$$G_u = exp\left[-exp\left(-\frac{\mu-b}{a}\right)\right] \tag{8}$$

Exponential model is the commonly used wind velocity profile model in engineering.

$$u/u_r = (z/z_r)^r \tag{9}$$

R is the wind speed profile index; Z and R are the reference height; UR is the average wind speed at the reference height.

The equivalent average wind speed at the driving height is mainly affected by two factors: (1) the wind speed is slightly increased by the flow around the bridge structure; (2) The effect of boundary layer and railing reduces the equivalent wind speed. The influence of the two factors is unified, and the ratio of the equivalent wind speed of the bridge deck to the incoming wind speed is defined as the influence coefficient Ks, then

$$\lambda_s = \frac{ueff}{u(zd)} \tag{10}$$

U (z D) is the incoming wind speed of the bridge deck height z D. For the main girder deck, the effect of the acceleration around the flow is smaller than that of the boundary layer and the railing, and usually Ks < 1. In the vicinity of the bridge tower, due to the great influence of the acceleration of the flow around the bridge tower, Ks > 1 is generally used. The influence coefficient Ks was determined by wind tunnel model test, which was carried out in TJ-3 atmospheric boundary layer wind tunnel of Tongji University. The model included bridge tower and part of main girder, and the length and height of the model were 130.5 m and 55.5 m respectively for the real bridge area.

The relationship between the equivalent wind speed of the bridge deck and the meteorological observation wind speed of the bridge at the reference height is established as follows:

$$u_r = \frac{z_r u_{eff}}{zD\lambda s} \tag{11}$$

The following is a specific calculation and analysis of the three typical vehicles on a sea bridge under the above dangerous conditions. Although the car is affected by the interference force is

ISSN: 2692-7608 DOI: 10.6981/FEM.202108_2(8).0027

small, but its load is small, so the adhesion limit is small, in the above several working conditions, prone to dangerous situations. Due to the large windward area of the bus, under the action of the wind, by the disturbance force is large, more dangerous. Container semi-trailer windward area is also large, the wind under the influence of interference is also large, and in the crosswind under the effect of folding phenomenon may occur, more dangerous. According to the requirements of driving safety, dynamics analysis is carried out to calculate the limit wind speed of safe driving under various dangerous conditions on the bridge deck. In other words, if the wind speed exceeds this limit, driving safety cannot be guaranteed. The table below shows the calculated ultimate wind speed of safe driving under various dangerous working conditions (taking the design height of the bridge H =45 m, R =1 000 m,α= 2%, α '= 2% as the basis)

Tab. 3 Topmost wind speed for driving safety in all circumstance

Models	Speed	Limit speed on crosswinds and curves					Windward and leeward uphill safe driving limit wind speed								Crosswind stable and safe running speed
		Crosswind driving limit				Lateral tilting	Windward uphill driving limit				Leeward slope braking				
		ICE	snow	Wet asphaltcement			ICE	snow	Wet asphaltcement		ICE	snow	Wet asphaltcement		$\omega_r < 3°\cdot s^{-1}$
Cars	40	12	21	40	48	＞55	＜0	18	58	73	20	37	72	84	31
	100	＜0	9	37	45	＞55	＜0	3	43	55	20	37	72	84	21
bus	40	16	27	52	＞55	＞50	6	43	118	152	35	59	111	129	24
	100	＜0	14	50	＞55	＞50	＜0	26	102	135	35	59	111	129	16
container	40	12	19	36	43	39	＜0	9	88	133	4	30	67	78	32
	100	＜0	10	33	41	37	＜0	＜0	72	116	4	30	67	78	21

Based on the data in the table and various dangerous working conditions, the following suggestions can be summarized to ensure the safety of traffic of various vehicles on the sea bridge.

On the ice road, due to the upwind uphill driving conditions can not be met, the bridge should be sealed until the bridge surface is frozen and cleared.

On the snow road, due to the limit condition of upwind uphill driving, the bridge surface wind force is greater than 9 m·s-1(equivalent to the basic wind speed level 4 wind force), the bridge should be closed until the snow is cleared. When there is snow on the bridge, but the wind speed on the bridge is less than 9 m·s-1(equivalent to the basic wind speed of grade 4 wind), cars can travel on the bridge at a speed less than 40 km·h-1.

For the general dry and wet road surface, if only considering the ultimate safety (such as exceeding the adhesion limit and side roll-over, etc.), the car can drive on the bridge deck at a speed less than 100 km· h-1 within the wind speed range of 35 m·s-1(equivalent to the basic wind speed of wind force 10).

If the safety of vehicles on the bridge deck is considered from the perspective of crosswind stability, the yaw Angle velocity ωr<3°·s-1 is taken as the standard. In order to ensure the crosswind driving stability, the bridge deck wind speed is required to be less than 24 m·s-1(equivalent to the basic wind speed level 7 wind force) and the vehicle speed to be less than 40 km· h-1.

5. Conclusion

In this paper, the static model is used to analyze the safety crosswind wind speed standards of four representative vehicle types. The results show that the crosswind safety of sedan vehicles is the best, followed by no-load medium buses and container trailers, and the crosswind safety

ISSN: 2692-7608 DOI: 10.6981/FEM.202108_2(8).0027

of minivan is the worst. Considering the analysis results, it is suggested that the equivalent wind speed of the bridge deck is equal to 20 m/s as the safe wind speed standard of the bridge deck.

Based on the meteorological observation data of the bridge location and the influence analysis of the bridge structure on the equivalent wind speed of the bridge deck, the probability evaluation method for the traffic safety of the bridge deck was established. The probability evaluation method is applied to Hangzhou Bay Cross-sea Bridge and Sutong Yangtze River Highway Bridge to compare the driving safety probabilities of the two Bridges, and the following conclusions are drawn:

(1) The bridge traffic safety problems are mainly concentrated near the main tower, and become serious with the increase of the width of the main tower.

(2) The possibility of safe driving across Central Africa is small, and the time of possible danger is about 13~15h each year (within 13~15d respectively).

(3) There are three main factors affecting the safety of the bridge deck, that is, the wind environment of the bridge site, the height of the bridge deck and the bridge structure. The more frequent and greater the wind speed at the bridge, the worse the driving safety. The higher the bridge deck is, the worse the driving safety is. The more blunt the bridge structure is, the greater the bridge deck wind speed is. The more railings on the bridge deck, the smaller the wind speed on the bridge deck, the more conducive to safe driving.

References

[1] Jiao Ao, Shen Yongjiang, Wang Zhengyang, Chen Tao, Tao Haowen, Xu Zhisheng, Fan Chuangang. Experimental study on the effect of canyon cross wind yaw angle on airflow and flame characteristics in a tunnel [J]. Journal of Wind Engineering & Industrial Aerodynamics, 2021,213{5}:

[2] Kocoń Agnieszka, Flaga Andrzej. Critical velocity measurements of freight railway vehicles roll-over in wind tunnel tests as the method to assess their safety at strong cross winds[J]. Journal of Wind Engineering & Industrial Aerodynamics, 2021,211{5}:

[3] Tingzhen Ming, Yongjia Wu, Renaud K. de_Richter, Wei Liu, S.A. Sherif. Solar updraft power plant system: A brief review and a case study on a new system with radial partition walls in its collector[J]. Renewable and Sustainable Energy Reviews, 2017,69{5}:

[4] Jing Zeng, Lai Wei, Pingbo Wu. Safety evaluation for railway vehicles using an improved indirect measurement method of wheel–rail forces [J]. Journal of Modern Transportation, 2016,24(2):

[5] Derek Bradley, Philip H. Gaskell, Xiaojun Gu, Adriana Palacios. Jet flame heights, lift-off distances, and mean flame surface density for extensive ranges of fuels and flow rates[J]. Combustion and Flame, 2016,164{5}:

[6] M.A. Moghimi, K.J. Craig, J.P. Meyer. Optimization of a trapezoidal cavity absorber for the Linear Fresnel Reflector [J]. Solar Energy, 2015,119{5}:

[7] H. Reshadatjoo, S. Yekani Moltagh, I. Mirzayi. Numerical investigation of the performance of Heller typecooling towers in different arrangements from the perspective of air intake flowrate [J]. Mechanics & Industry, 2015,16(6):

[8] Y.B. Zhao, Guoqing Long, Fengzhong Sun, Yan Li, Cuijiao Zhang. Numerical study on the cooling performance of dry cooling tower with vertical two-pass column radiators under crosswind[J]. Applied Thermal Engineering, 2015,75{5}:

[9] Wang, Wen, Chen. Simulation of Large-Scale LNG Pool Fires Using FireFoam[J]. Combustion Science and Technology, 2014,186(10-11):